Supplementary Information for

Microbiome-assisted carrion preservation aids larval development in a burying beetle

Shantanu P. Shukla, Camila Plata, Michael Reichelt, Sandra Steiger, David G. Heckel, Martin Kaltenpoth, Andreas Vilcinskas, and Heiko Vogel

SI Results

Fig. S1 (A) A breeding *Nicrophorus vespilloides* adult tending to its larvae housed in the feeding cavity of a prepared carcass. (B) Final instar larvae removed from their carcass. (C) Fresh mouse cadavers were assigned to either 'tended' or 'untended' categories. For the untended category, cadavers were cut open using a sterile blade near their abdomen to match the feeding cavity of tended carcasses. (D) The cadavers were then buried using sterile swabs to make them comparable to beetle-tended carcasses. (E) Cotton swabs were used to sample the carcass-matrix for analyzing the microbiome, metatranscriptome and the carcass' biochemical properties. Carcasses were also swabbed to remove the carcass matrix, to test the effect of the carcass microbiome on beetle fitness. The swabs on the left and right indicate before and after swabbing beetle-tended carcasses, with the dark-brown matrix collected from the cavities of tended carcasses seen attached to the cotton swab. (Photos by Shantanu Shukla)

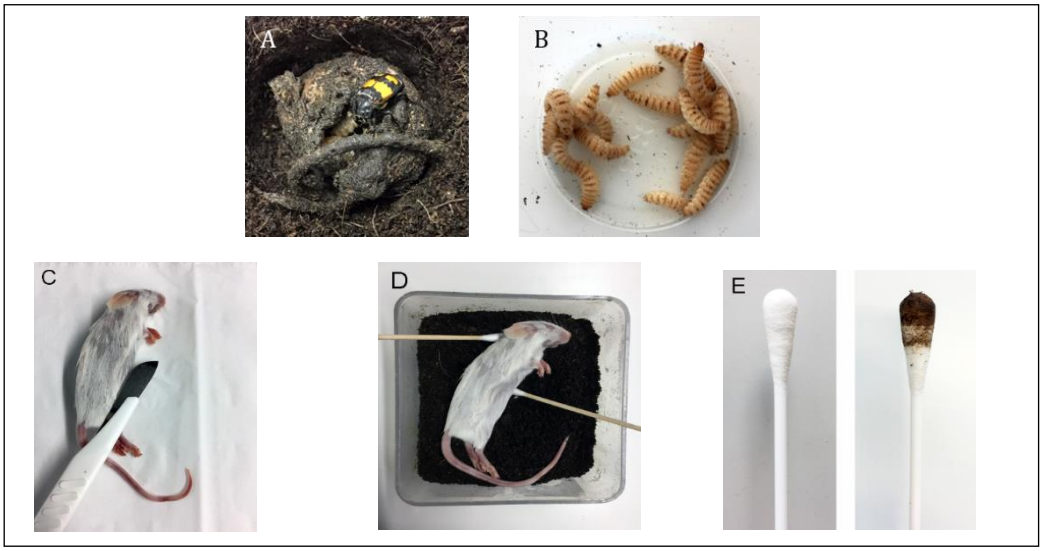

www.pnas.org/cgi/doi/10.1073/pnas.1812808115

Fig. S2 Taxonomic composition of bacterial communities associated with soil, *N. vespilloides* tended and untended carcasses. Proportion of bacterial phyla plotted for each sample.

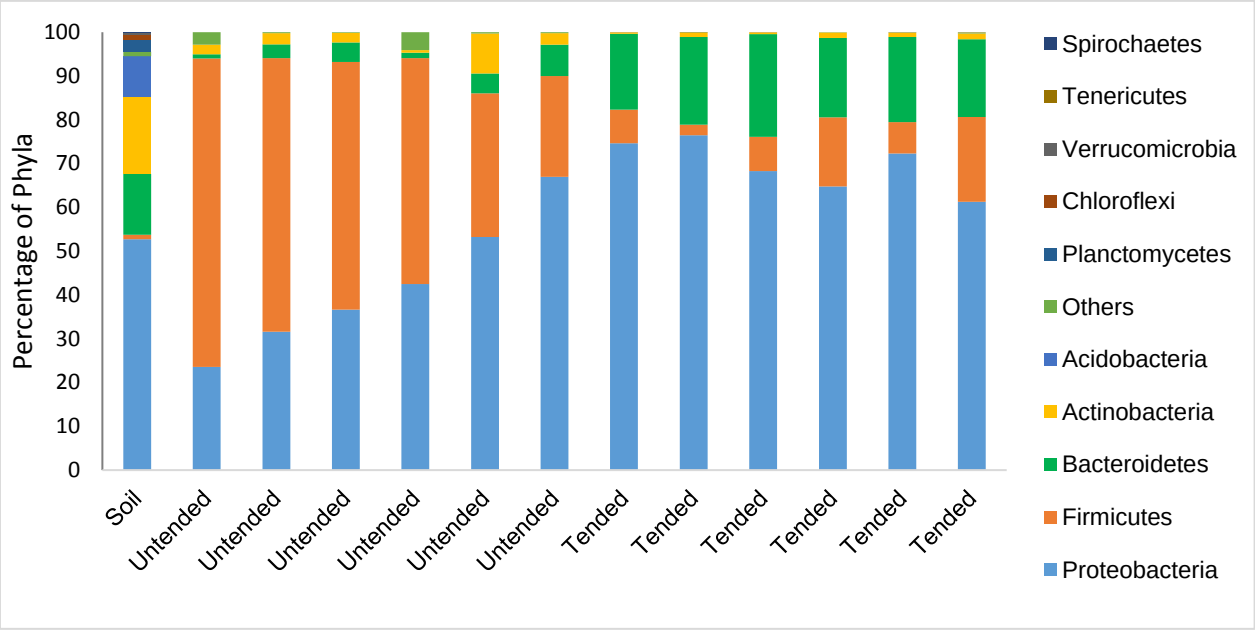

Fig. S3 Fungal community composition of tended carcasses, untended carcasses, and soil with relative abundance of sequences summarized at the genus level plotted as a heatmap.

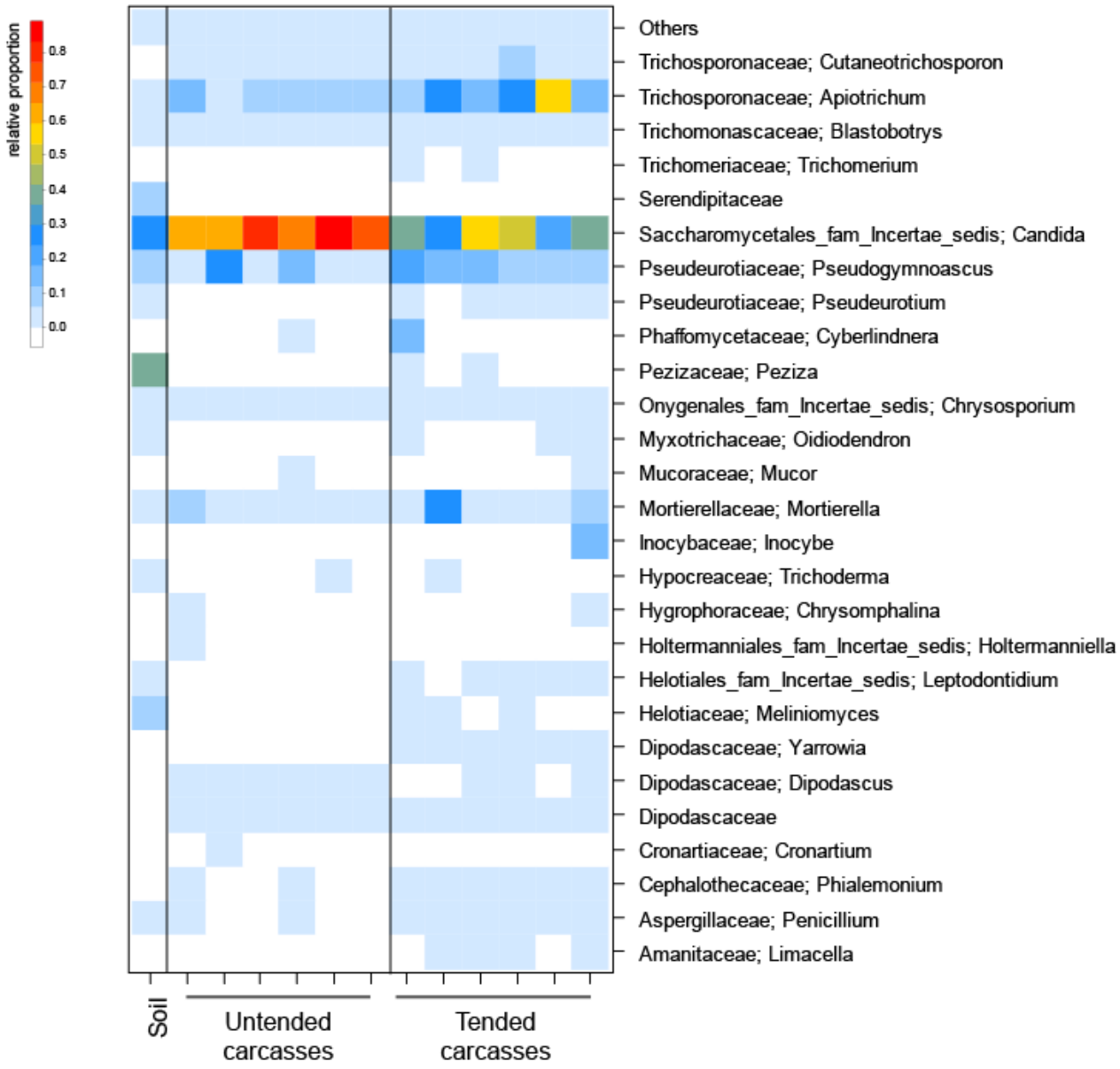

Fig. S4 Biological community distribution of transcripts (uncurated results from the polyA+ enriched mRNA dataset) sampled from *N. vespilloides* tended carcasses and untended carcasses. Tended carcasses had relatively higher abundance of transcripts assigned to nematodes, followed by the yeast *Yarrowia*. However, higher nematode-originating transcripts could arise due to their greater relative biomass, and may not necessarily reflect higher metabolic activity. Green bars indicate transcripts assigned to nematodes, blue to bacteria, red to fungi, and brown bars indicate others.

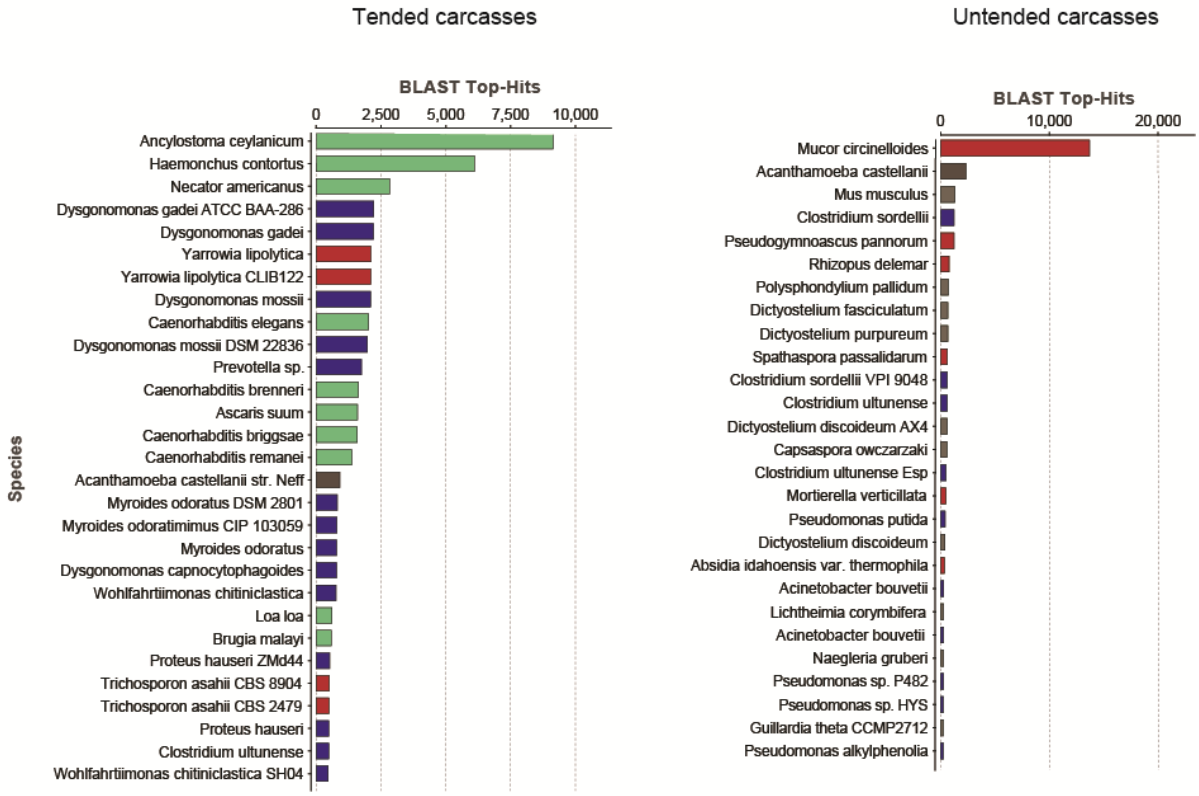

Fig. S5 Visualization of protease and lipase activity using agar diffusion assays. (A) Skim Milk Agar was used to test for protease activity, and (B) Tributyrin Agar was used to test for lipase activity. UC=untended carcass, TC=tended carcass, P=positive control (pure protease or lipase enzyme, see SI Methods), N=negative control (phosphate buffered saline).

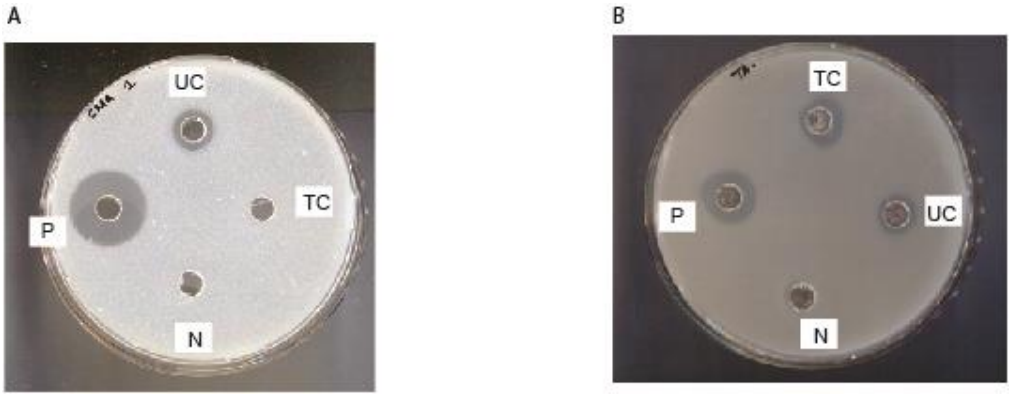

Fig. S6 Quantification of total lipase activity in tended (n=7) and untended (n=7) carcasses. Different letters indicate significant differences. Results based on Wilcoxon rank-sum test, p=0.023.

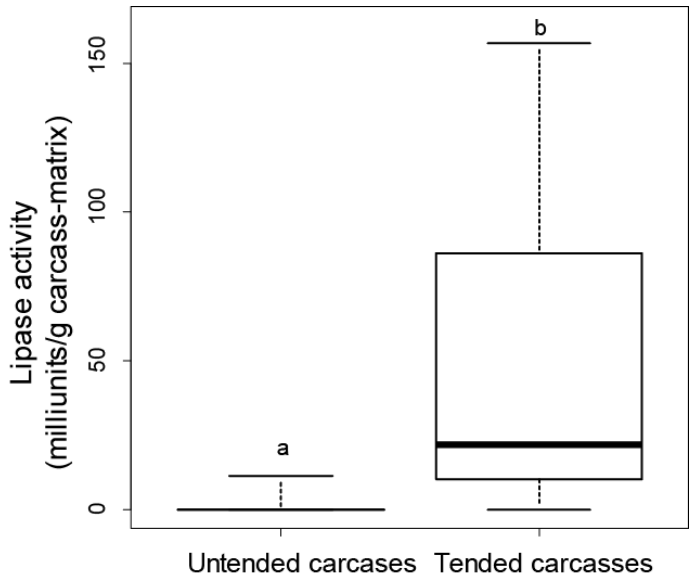

Fig. S7 Effect of carcass matrix on larval development. (A) Removal of carcass matrix resulted in lower average larval weight per brood. (B) There was no difference in the number of larvae produced per brood between the two groups. Average values per brood for each treatment are plotted. Different letters above standard error whiskers indicate significant differences using t-test, alpha=0.05.

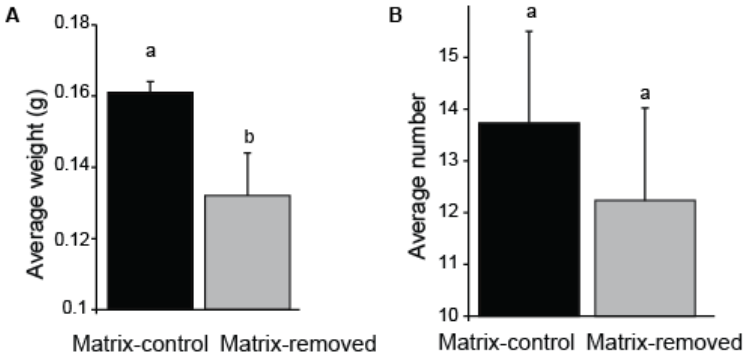

Table S1 Alpha diversity measures for bacterial and fungal communities based on 16S rRNA and ITS1 amplicon sequencing.

Number	Sample type	Bacteria (16S rRNA sequences)			Fungi (ITS sequences)
		Shannon index average (± SD)	Faith's phylogenetic diversity average (± SD)	Evenness average (± SD)	Shannon index average (± SD)
1	Tended carcass	3.7 (0.41)	4.5 (1.2)	0.6 (0.06)	3.7 (0.5)
2	Untended carcass	3.2 (0.83)	5.7 (2.9)	0.5 (0.11)	3.2 (0.1)
3	Soil	6.6	12.2	0.8	3.47

Table S2 Bacterial genera identified to be differentially abundant between tended and untended carcasses using analysis of composition of microbiomes (ANCOM). The relative abundance (percentage) for each genus per group is listed below. Only those bacterial features for which the null hypothesis is rejected are reported.

Bacterial feature	Untended carcasses	Tended carcasses	W	Reject null hypothesis
Pseudomonas (Pseudomonadaceae)	17.7	0.2	53	True
Staphylococcus (Staphylococcaceae)	4.8	0.01	64	True
Unclassified Sphingobacteriaceae	0.3	<0.01	51	True
Chitinophaga (Chitinophagaceae)	0.3	0.0	56	True
Aerococcus (Aerococcaceae)	0.3	0	56	True
Unclassified Alcaligenaceae	0.2	0	52	True
Vitreoscilla (Neisseriaceae)	0.3	31.0	59	True
Dysgonomonas (Porphyromonadaceae)	0.05	10.2	66	True
Providencia (Enterobacteriaceae)	0.01	2.0	67	True
Myroides (Flavobacteriaceae)	0.04	7.5	61	True
Unclassified Lactobacillales	0.01	1.4	58	True
Serratia (Enterobacteriaceae)	0	0.8	65	True

Table S3 Identification of differentially abundant fungal genera between untended and tended carcasses using ANCOM. Out of 104 unique fungal genera tested, only one genus (*Yarrowia*) was significantly different between the two groups. Relative abundance (percentage) of the genus for each group is listed below. *Yarrowia* had significantly higher relative abundances in tended carcasses as compared to untended carcasses.

Fungal genus	Untended carcass	Tended carcass	W	Reject null hypothesis
Yarrowia	0.1	0.6	145	True

Table S4 Characterization of the fungal community of untended and tended carcasses. Fungal sequences were obtained by cloning amplification products of the LS1/LR5 primers, which target the partial fungal large subunit (LSU) rRNA region. The genus *Yarrowia* was highly abundant in tended carcasses and absent from most untended carcass samples. Non-fungal sequences were excluded from the analysis. Samples U1 to U5 represent untended carcasses, and T1 to T6 represent tended carcasses. The last two columns represent the proportion of sequences for each genus (as percentage values) for pooled untended and tended carcasses respectively.

Genus	**U1**	**U2**	**U3**	**U4**	**U5**	**T1**	**T2**	**T3**	**T4**	**T5**	**T6**	**Untended (percent)**	**Tended (percent)**
Apiotrichum	2	0	0	0	0	0	0	0	0	0	0	5.1	0.0
Candida	10	4	5	1	1	0	0	0	0	0	1	53.8	3.0
Galactomyces	0	0	0	0	1	0	0	0	0	0	0	2.6	0.0
Gymnostellatospora	3	0	0	0	0	0	0	0	0	1	0	7.7	3.0
Pseudogymnoascus	2	0	0	0	0	0	0	0	0	0	0	5.1	0.0
Scheffersomyces	3	1	0	1	2	2	0	0	0	0	0	17.9	6.1
Trichosporon	0	2	0	0	0	0	0	0	0	0	0	5.1	0.0
Yarrowia	**1**	**0**	**0**	**0**	**0**	**4**	**2**	**17**	**1**	**4**	**1**	**2.6**	**87.9**
Others	6	0	0	0	1	0	0	0	0	0	0	17.9	0.0
Total	21	7	5	2	4	6	2	17	1	5	2	100.0	100.0

Table S5 GO term analysis of differentially abundant transcripts (ten-fold change or higher) with significantly higher representation in tended carcasses as compared to untended carcass samples. GO terms are summarized at level 4. Only significantly overrepresented GO terms are listed (FDR corrected p-values < 0.05).

GO ID	GO Name
GO:0071852	fungal-type cell wall organization or biogenesis
GO:0051984	positive regulation of chromosome segregation
GO:0044182	filamentous growth of a population of unicellular organisms
GO:0042710	biofilm formation
GO:0051983	regulation of chromosome segregation
GO:0090068	positive regulation of cell cycle process
GO:0044011	single-species biofilm formation on inanimate substrate
GO:0030435	sporulation resulting in formation of a cellular spore
GO:0043934	sporulation
GO:0051304	chromosome separation
GO:0030437	ascospore formation
GO:0044770	cell cycle phase transition
GO:0036180	filamentous growth of a population of unicellular organisms in response to biotic stimulus
GO:0034293	sexual sporulation
GO:0043935	sexual sporulation resulting in formation of a cellular spore
GO:0044407	single-species biofilm formation in or on host organism
GO:0071555	cell wall organization
GO:0044107	cellular alcohol metabolic process
GO:0000746	conjugation
GO:0032506	cytokinetic process
GO:0009405	pathogenesis
GO:0045229	external encapsulating structure organization
GO:0051038	negative regulation of transcription involved in meiotic cell cycle
GO:0009414	response to water deprivation
GO:0090033	positive regulation of filamentous growth
GO:0036171	filamentous growth of a population of unicellular organisms in response to chemical stimulus
GO:0009415	response to water
GO:0001539	cilium or flagellum-dependent cell motility
GO:0010570	regulation of filamentous growth
GO:0000747	conjugation with cellular fusion
GO:0051666	actin cortical patch localization
GO:0007114	cell budding
GO:0045787	positive regulation of cell cycle
GO:0045023	G0 to G1 transition
GO:0044116	growth of symbiont involved in interaction with host
GO:0031321	ascospore-type prospore assembly

Table S6 GO term analysis of differentially abundant transcripts (ten-fold change or higher) with significantly higher representation in untended carcasses as compared to tended carcass cavity samples. GO terms are summarized at level 4. Only significantly overrepresented GO terms are listed (FDR corrected p-values < 0.05).

GO ID	GO Name
GO:0046483	heterocycle metabolic process
GO:1901135	carbohydrate derivative metabolic process
GO:0006793	phosphorus metabolic process
GO:0006520	cellular amino acid metabolic process
GO:0015980	energy derivation by oxidation of organic compounds
GO:0044723	single-organism carbohydrate metabolic process
GO:0010604	positive regulation of macromolecule metabolic process
GO:0005975	carbohydrate metabolic process
GO:0070887	cellular response to chemical stimulus
GO:0019080	viral gene expression
GO:1901615	organic hydroxy compound metabolic process
GO:0006979	response to oxidative stress
GO:0006099	tricarboxylic acid cycle
GO:0006790	sulfur compound metabolic process
GO:0019725	cellular homeostasis
GO:0009636	response to toxic substance
GO:0033554	cellular response to stress
GO:0098869	cellular oxidant detoxification
GO:0044262	cellular carbohydrate metabolic process
GO:0051172	negative regulation of nitrogen compound metabolic process
GO:0072593	reactive oxygen species metabolic process
GO:0006081	cellular aldehyde metabolic process
GO:0019538	protein metabolic process
GO:0010035	response to inorganic substance
GO:0042180	cellular ketone metabolic process
GO:0006575	cellular modified amino acid metabolic process
GO:0000746	conjugation
GO:0010033	response to organic substance
GO:0097164	ammonium ion metabolic process
GO:1901700	response to oxygen-containing compound
GO:0055114	oxidation-reduction process
GO:0009991	response to extracellular stimulus
GO:0071852	fungal-type cell wall organization or biogenesis
GO:0031647	regulation of protein stability
GO:0015977	carbon fixation
GO:0006020	inositol metabolic process
GO:1901575	organic substance catabolic process
GO:0045454	cell redox homeostasis

GO:0080135	regulation of cellular response to stress
GO:0009408	response to heat
GO:0019637	organophosphate metabolic process
GO:0046999	regulation of conjugation
GO:0009266	response to temperature stimulus
GO:0007584	response to nutrient
GO:0045833	negative regulation of lipid metabolic process
GO:0006486	protein glycosylation
GO:0016237	lysosomal microautophagy
GO:0042594	response to starvation
GO:0034369	plasma lipoprotein particle remodeling
GO:0035966	response to topologically incorrect protein
GO:0070085	glycosylation
GO:0045595	regulation of cell differentiation
GO:0009410	response to xenobiotic stimulus
GO:0045913	positive regulation of carbohydrate metabolic process
GO:0007571	age-dependent general metabolic decline
GO:0061635	regulation of protein complex stability
GO:0043094	cellular metabolic compound salvage
GO:0019400	alditol metabolic process
GO:0044770	cell cycle phase transition
GO:0034975	protein folding in endoplasmic reticulum
GO:0006805	xenobiotic metabolic process
GO:0006952	defense response
GO:0051668	localization within membrane
GO:0046937	phytochelatin metabolic process
GO:0060263	regulation of respiratory burst

Identification of the carcass-associated fungus

The fungus growing on untended carcasses was identified to belong to the genus *Mucor*, with high similarity to *Actinomucor elegans* and *Mucor moelleri*.

The partial fungal large-subunit (LSU) ribosomal RNA gene sequence is as follows:

AGTCTTTCGCCCCTATACCCAAATTTGACGATCGATTTGCACGTCAGAATCGCTACGAGCCTC
CACCGGAGTTTCCTCCGGCTTCACCCTATTCAGGCATAGTTCACCATCTTTCGGGTCCCATCA
TAAGTGCTTTACCTCGGTCACTTCTGTATAAAACGTCGACGCCGGGTGATACTGCCATCCCAA
AGGGACTTGGTATCCATCAGTTTCCTTACGCGTATGGGTTTGGCACCCAAACACTTGCACTTA
TGGTGGACTCCTTGGTCCGTGTTTCAAGACGGGTCATTTAGAGTCATTAAGCCAACAACCTAA
GCGAATAAAAAATATACAGCGCGGGTTCCACCTTTAAACACTAGCACCACCCGAAGCAGAA
ATTCTAGCATTTATCAGCGAAAGCACGCCGCAATCTCGCCTAATGGCATTCGCTGCGATCCTC
AGTCCAATCCAGGGTATTTTCCAAGAGGCTATAACACCCCCTAAGGGGCCACATTCCGCCTG
GTTTTTTCCCCCAAATAAAACTGTCGTTGGCAGGCATAGGCCGCAAGTGCATCCGGGCAAAA
GCCCAGATTGATTACAGCCAAGCCAGTCTGGCTCCAAACGGTTCCCTTTTAACAATTTCACAT
ACTGTTTAACTCTCTTTTCAAAGTTCTTTTCATCTTTCCCTCACGGTACTTGTTCGCTATCGGTC
TCTCGCCAATATTTAGCTTTAGGTGAGATTTACCACCCAATTTAGGCTGCATTCCCAAACAAC
CTGACTCTTTGAAAGTGTATCGCAAAAGACAACTGCTCAGGCCAAAGACGGGATTCTCACCC
TCTATGATGCCCTGTTCCAAAGGACTTTTTTGCCTGGCGTGTCAGGAAAACACTTCTACAGTT
TACAATCCGGCTTGGCTAAGCCAAGCAGGTTCCAACTTTGAGCTCTTTCCTCTTCACTCGCCG
TTACTGGGGAA

SI Methods

Beetle rearing

The burying beetle *N. vespilloides* Herbst was cultured in laboratory incubators (20 ˚C, 80% relative humidity and a 16-h photoperiod) in plastic boxes containing garden soil and fed with larvae of *Tenebrio molitor* (one larva per adult, twice a week) until sexual maturity (>20 days post eclosion). To enable breeding, sexually mature, virgin males and females from different families were paired together (one pair each box) and provided with a frozen mouse cadaver (*Mus musculus*; b.t.b.e Insektenzucht GmbH, Schnürpflingen, Germany), thawed at room temperature 3–4 h before the experiment.

Experimental setup

Mouse cadavers weighing 15-20 grams were randomly assigned to either 'untended carcasses' that had no contact with the beetles, or 'tended carcasses' that were provided to a pair of sexually mature beetles. Plastic boxes that housed the beetles were cleaned, disinfected and filled with fresh, non-sterile garden soil prior to use. Because beetles create an opening in the carcass for the larvae to enter and feed, we used sterile scalpels (Braun, Tuttlingen, Germany) to make incisions in the abdomen of untended cadavers (before contact with the soil) to match tended carcasses. Carcasses were monitored daily. To maintain consistency, untended carcasses were then buried using sterile swabs (Sarstedt, Germany), once tended carcasses were seen to be buried by the breeding beetles. Both carcass groups were sampled once tended carcasses housed actively feeding third instar larvae, nine days after the start of the experiment, but prior to the larvae migrating away from the carcass, making the comparisons ecologically relevant. The beetle-prepared cavities of tended carcasses and artificially created cavities of untended carcasses were sampled using sterile, DNA-free swabs (Sarstdedt, Germany) by rotating the swabs inside the cavity for 10 seconds and were immediately transferred into tubes for extraction of DNA and RNA, enzyme assays or polyamine quantification (see below). For untended carcasses, the swabbed region corresponded to the cavity created by the artificial incision. This included sampling around the inner tissue and the intestines of the cadaver. For tended carcasses, this included sampling the inner lining of the feeding cavity, a region created by the consumption of the carcass' internal tissue by the larvae and adult beetles. Prior to sampling, soil and debris from the external surface were removed from both tended and untended carcasses using sterile cotton swabs. The larvae and adults were temporarily removed from the cavity of tended carcasses during sampling. Carcasses were sampled in a clean, sanitized area using disinfected laboratory gloves to avoid contamination.

Processing of 16*S* rRNA and ITS sequence data

The 16*S* rRNA amplicon sequence data were analyzed using QIIME2 (v2017-09) (1) (https://qiime2.org). Paired sequences (obtained from Illumina MiSeq platform) were demultiplexed, denoised using DADA2 (2) (in QIIME2) after truncating all sequences at 240 nucleotides based on sequence quality profiles. Chimeras were removed using the default 'consensus' method. Unique sequences were aligned using MAFFT (3), filtered using the default mask alignment file, and were used to construct a phylogeny using FastTree (4). Alpha diversity measures (Shannon's diversity, observed OTUs, and Faith's phylogenetic diversity) and beta diversity measures (binary Jaccard's distances, Bray-Curtis dissimilarity, and unweighted UniFrac distances) (5, 6) were estimated using a subsampled feature table containing 19,400 sequences per sample. Taxonomy was assigned using a Naïve Bayes classifier trained on the GreenGenes database (7) (version 13_8) using trimmed sequences pre-clustered at 99% similarity. Principal coordinates analysis was performed on beta diversity measures using Emperor (8). We used analysis of composition of microbiomes ANCOM (9) to test differences in the abundances of bacterial taxa between tended and untended carcasses. ANCOM tests the null hypothesis that taxon abundance between two

ecosystems/sample categories are equal on average and compares the relative abundance of a taxon between two groups using log-ratio abundance values. Sequence taxa were summarized at the genus level for the analysis.

Fungal ITS (internal transcribed spacer) amplicon sequencing data were analyzed using QIIME2 (v2017.12) and QIIME1 v1.9.1. The fastq file containing the forward reads (obtained from the Illumina MiSeq platform) was used as follows. Primers and barcodes were removed using cutadapt (10). Sequences were denoised and quality filtered (minimum quality score = 20) using DADA2 in QIIME without length truncation, using default parameters. Chimeras were removed using the 'consensus' method. High-quality ITS1 sequences were used for downstream analyses. Taxonomy was assigned using the QIIME2 feature-classifier plugin and the Naïve Bayes classifier trained on the 'dynamic' reference files from the 'developer' version of the UNITE ITS database v7.2 (release date 1.12.2017) (11), with the confidence parameter set to 0. Differentially abundant fungal sequences were identifies using ANCOM (analysis of composition of microbiomes). Dissimilarities in fungal communities of tended and untended carcasses were tested using ANOSIM (analysis of similarities). The abundance table was uniformly rarefied at 40,000 sequences per sample for alpha and beta diversity comparison. Heatmaps were plotted using the *lattice* package (12) in *R* v3.4.2 (13). Alpha diversity (Shannon index) between tended and untended carcasses was compared using a pairwise Kruskal-Walis test with p values based on the Benjamin-Hochberg correction.

Characterization of the fungal community using cloning of partial fungal LSU sequences

Individual samples from untended carcasses (n=5) and tended carcasses (n=6) were used for amplification of a 900 bp region of the fungal large subunit (LSU) rRNA gene using the primers LS1 and LR5 (14-16). A 20 µl PCR reaction was set up using thermocycler conditions as described previously (17, 18). PCR products were purified using a Zymo Clean and Concentrator 5 kit (Zymo Research) and cloned into competent *Escherichia coli* cells using the TOPO TA cloning kit (containing the PCR4-TOPO vector) according to the manufacturer's protocol (Invitrogen). Plasmid DNA was isolated using a DNA isolation kit (Nexttec) and processed using the BigDye Terminator v3.1 cycle sequencing kit (Applied Biosystems). Sequencing proceeded with the M13fwd primers on a 3730xl DNA Analyzer. Reads were quality trimmed using Geneious (v9.1.3). Only those sequences with length greater than 100 bases (after trimming) were included in the analysis. Sequences were identified using megaBLAST against the NCBI nr database. Sequences having hits against the cloning vector or against non-fungal organisms (nematodes) were excluded from the analysis.

Carcass metatranscriptomic analysis: RNA extraction and RNA-Seq analysis

To characterize microbial metabolism on carcasses and to investigate their potential contribution to carcass degradation, we sampled the cavities of tended and untended carcasses using sterile DNA-free swabs as described in the Methods section. The swabs were immediately transferred into TRIsure (Bioline) and frozen in liquid nitrogen. Total RNA from the carcasses was extracted as described previously (18). Briefly, sample swabs were homogenized in a TissueLyzer (Qiagen, Hilden, Germany), and RNA was extracted using bromo-3-chloropropane, precipitated in isopropanol, washed with 80% ethanol, and suspended in nuclease-free water (Thermo Fisher Scientific). DNA was digested with TurboDNase (Thermo Fisher Scientific), and purified using RNA Clean and Concentrator 5 (Zymo Research). RNA quality was checked with a RNA 6000 nano LabChip kit using a 2100 Bioanalyzer (Agilent Technologies). Total RNA was depleted for rRNAs using the Ribo-Zero rRNA Removal Kit (Illumina) and subsequently poly(A)$^+$ mRNAs were isolated using the TruSeq RNA Library Prep Kit (Illumina). The poly(A)$^+$ mRNA fraction was used to construct the eukaryotic cDNA library while the remaining non-captured poly(A)$^-$ mRNA was used for the prokaryotic cDNA library. A total of 12

samples were sequenced by the Max Planck Genome Center Cologne (MPGCC) on an Illumina HiSeq2500 Genome Analyzer platform, using paired-end (2 x 125 bp) reads. This yielded approximately 30 million reads for each feeding cavity sample. Quality control measures, including the filtering of high-quality reads based on the score given in fastq files, removal of reads containing primer/adapter sequences, and trimming of read length, were carried out using CLC Genomics Workbench v9.1 (https://www.qiagenbioinformatics.com).

For the eukaryotic and prokaryotic *de novo* transcriptome assemblies, data from the three replicate samples were pooled. Subsequently, individual samples were mapped independently to the transcriptome assembly. Differences in sequence datasets and transcript sizes were corrected using the RPKM algorithm (reads per kilobase of transcript per million mapped reads) to obtain correct estimates for relative expression levels for each replicate. Log2 (RPKM) values (normalized mapped read values; geometric means of the biological replicate samples) were subsequently used for calculating fold-change values. To identify differentially expressed transcripts, untended carcasses and tended carcasses (n=3 for each group) were compared using a Student´s t-test corrected for multiple testing using the Benjamini–Hochberg procedure to control the false discovery rate (FDR).

Identification of relative abundance of bacterial and fungal transcripts: To determine the relative abundance of the dominant fungi and bacteria in carcasses, differentially abundant transcripts were separated based on those that were overrepresented in tended and untended carcasses. Because the eukaryotic RNAseq libraries contained many transcripts assigned to nematodes and other non-fungal organisms, the differentially abundant transcript dataset was manually curated to retain only known fungal genera, based on approximately 2900 fungal genera obtained from the NCBI taxonomy browser (accessed on 05-04-2018). This resulted in retaining 1,611 fungal transcripts out of 40,617 transcript contigs. Similarly, the prokaryotic dataset was manually curated to retain only bacterial reads by comparing against the NCBI taxonomy browser (accessed 19-03-2018) containing approximately 3500 bacterial genera.

Gene Ontology (GO) and InterPro terms (InterProScan, EBI), enzyme classification (EC) codes, and metabolic pathways (Kyoto Encyclopedia of Genes and Genomes, KEGG) (19) were carried out using BLAST2GO v4. 1 (http://www.blast2go.de). Digital gene expression analysis was carried out using CLC Genomics Workbench v9.1 to generate BAM (mapping) files, and QSeq Software (DNAStar Inc., Madison, WI, USA) was then used to estimate expression levels. Fisher's exact test was used as part of BLAST2GO to identify the overrepresentation of GO terms among lists of differentially expressed genes (ten-fold change or higher) between the tended and untended carcass cavity samples. The GO-enriched bar charts were simplified to display only the most specific GO terms by removing parent terms representing existing child terms using the function "Reduce to most specific terms" in BLAST2GO. A GO term was considered significantly enriched if the p-value corrected by FDR control was less than 0.05.

Identification of the carcass-associated fungus

The white mold from carcasses was isolated and purified on Yeast Malt Agar. Pure cultures were then inoculated in Yeast Malt Broth, and an aliquot of the culture was used for DNA extraction using the PowerSoil DNA extraction kit (Mo Bio, USA). Part of the fungal large subunit (LSU) rRNA gene was amplified using the primers LS1 and LR5 as described before. Amplicons were purified using a QIAquick gel extraction kit (Qiagen) and further amplified using the flanking primers M13fwd and M13rev and sequenced unidirectionally with M13fwd. The resulting sequence was analyzed and quality trimmed using Geneious (version 9.1.3) and the fungus was identified by comparing the sequence against the nr database using BLAST.

Quantification of biomass from carcass swabs

Swabs from the cavities of tended and untended carcasses were transferred to sterile 15 ml tubes containing 1.5 ml ice-cold MilliQ water. Tubes were vortexed (15 s at medium intensity) to dislodge the adhered matrix into the water. The swabs were then squeezed inside the tube to recover as much of the suspension before discarding. The tubes were weighed before and after the addition of the swabs to estimate amount of carcass biomass that was dislodged in the water. Samples were kept in ice throughout. To account for the mass of water from the suspension, a blank swab was immersed into similar tubes (n=2) and the tubes were weighed after removal of the cotton swabs. The average weight of the blank tubes (containing water only) was subtracted from all sample tubes to estimate the sampled carcass-matrix biomass. All suspensions were then filtered using a 0.45-µm filter (Carl Roth, Germany). The filtrate obtained from this procedure was used for quantifying protease concentrations, lipase activity, polyamine concentrations and free amino acid levels (represented per gram carcass biomass). This normalization was performed to account for differences in the collection of biomass, which could arise from differences in the texture of the matrix between tended and untended carcasses, or differences arising from the amount of carcass matrix that adhered to, or which was dislodged from the swabs during sampling.

Enzyme assays

All samples were assayed in duplicates using 5 µl of the carcass suspensions. Total lipase activity from tended carcasses (n=7) and untended carcasses (n=7) was estimated using the fluorometric Lipase Activity Assay Kit III (Sigma-Aldrich) according to the manufacturer's instructions. Lipase activity was estimated using a coupled enzyme reaction by measuring the generation of methylresorufin, which is proportional to enzymatic activity in the samples, by providing a lipase substrate and serial dilution of methylresorufin to plot a standard dose response. Total protease concentrations from tended carcasses (n=13) and untended carcasses (n=7) were estimated using the Pierce Fluorescent Protease Assay Kit (Thermo Fisher Scientific) according to the manufacturer's instructions. Protease concentrations in the sample were estimated based on a standard curve consisting of serial dilutions of Trypsin (0 – 500 ng/mL). Assays were performed using a Tecan Infinite200 plate spectrophotometer. Enzyme activity was compared between tended and untended carcasses using a Wilcoxon rank-sum test in *R*. In the agar diffusion assays, lipase activity was tested by adding 20 µl each of filtered suspension from untended and tended carcasses into wells bored in prepared Triglyceride Agar (VWR, USA), and protease activity was similarly tested using Skim Milk Agar. The plates also contained positive controls: 10 µg proteinase K (Thermo Fisher) on Skim Milk Agar, and 10 µg purified lipase from *Candida rugosa* (Sigma). Results were recorded after the plates were incubated at 25 ˚C for 24 h.

Skim Milk Agar composition: 2.8% low-fat milk powder (Roth), 0.5% casein hydrolysate, 0.25% yeast extract, 0.1% glucose, 1.5% agar. Final pH was adjusted to 7.0.

Carcass polyamine quantification

Putrescine and cadaverine were quantified from carcass swab filtrates as described above. For polyamine quantification, aliquots were analyzed as ortho-phthaldialdehyde/ethanethiol/fluorenylmethoxycarbonyl (OPA/Et/FMOC) derivatives (20). The extract was mixed in a ratio of 1:1 with 0.5 M potassium borate buffer (pH 11.0). Polyamines were derivatized using an Agilent G1313A autosampler by first mixing 50 µl of the alkaline sample with 50 µl of ortho-phthaldialdehyde/ethanethiol solution, i.e. 40 mg ortho-phthaldialdehyde (Sigma-Aldrich) and 200 µl ethanthiol (Sigma-Aldrich) in 10 mL of borate buffer (0.1 M, pH 11.0)/methanol 50:50 (v:v), for 1 min. For the second derivatization, 2 µl of 9-fluorenylmethoxy-carbonyl chloride (FMOC-Cl) (34 mg/ml acetonitrile) was added and incubated for 2 min. We then analyzed 30 µl of the double-derivatized samples by HPLC as described in the main article with the following gradient of solvent A (0.02 M sodium citrate buffer pH 5.5) and solvent B (methanol/acetonitrile 65:35 v:v) at a flow rate of 1.5 ml/min: 50% A/B; 50–100% B (0–10 min), 3-min hold 100% B, 100–50% B in 0.1 min, 50% B (1.5 min). Polyamines were quantified using calibration curves constructed with commercial standards of putrescine and cadaverine (Sigma-Aldrich). Putrescine and cadaverine concentrations were compared between tended and untended carcasses using the Wilcoxon rank-sum test in R.

Identification and quantification of free amino acids

Carcass swab filtrates (as described above) from tended and untended carcasses were analyzed by LC-MS using a Bruker Esquire 6000 ion trap mass spectrometer (Bruker Daltonics, Bremen, Germany) operated in alternating ionization mode in the *m/z* range 60–1000 (capillary exit voltage +117/–117 eV; capillary voltage +4,000/–4,000V; nebulizer pressure, 35 psi; drying gas, 11 L/min; gas temperature, 330°C) coupled to an Agilent 1100 series HPLC. Elution was accomplished using a Nucleodur Sphinx RP column (250 x 4.6 mm, 5 µm; Macherey- Nagel, Düren, Germany). The mobile phases were 0.2% formic acid (v:v) (A) and acetonitrile (B), starting with 100% A for 5 min, followed by a gradient to 45% B in 15 min. The subtraction of the mass spectrometer total ion chromatogram between tended and untended carcasses (using the software package Metabolite Detect 1.1, BrukerDaltonics, Bremen, Germany) identified differences between the two extracts. For relative quantification, peak areas of the ion traces for different compounds were extracted as follows: positive ionization mode: valine *m/z* 72+118; isoleucine *m/z* 86+132; leucine *m/z* 86+132; tyrosine *m/z* 165+182; phenylalanine *m/z* 120+166; tryptophan *m/z* 188+205. Peak areas pertaining to each amino acid were normalized by diving with the carcass biomass (mg) present in the sample.

Effect of carcass matrix on larval growth

Reproductively mature, virgin males and females from different families were paired and provided with a mouse cadaver to facilitate breeding. After pairing of the beetles, carcasses were monitored daily. Carcasses were randomly assigned to matrix-removed and matrix-control groups. For the matrix-removed group, the carcass-matrix from the feeding cavities of prepared carcasses was removed by sterile swabs once 1st instar larvae were seen on the carcass. Breeding adults (parents) and larvae were temporarily removed from the carcass, during the swabbing of the cavity. Multiple swabs were successively used to remove as much of the matrix present within the feeding cavity. This was done daily until larvae migrated away from the carcass in their pre-pupal phase. To maintain consistency, parents and larvae were also removed from the control group for the same amount of time as the treatment group, but without removal of the carcass matrix. In both groups, all larvae and parents were replaced back on the carcass. Beetle pairs that did not produce eggs were excluded from the experiment. Because removal of young larvae from the carcass could be stressful, only those larvae that survived at least one day after the start of the sampling were included in the analysis. Larvae were weighed individually from each brood, and the average value per brood, the maximum value per brood (max. larva), and the total number of larvae produced per brood

were analyzed. Because larval biomass and numbers can be influenced by the size of the carcass and the amount of food consumed, we weighed the mouse cadaver before start of the experiment (before providing it to the breeding adults) and at the end of the experiment (when all larvae had migrated away from the carcass, indicating end of the feeding stage). Adherent soil from consumed carcasses was removed prior to weighing. The difference in the weights of the carcass on the two days was used to calculate the amount of carcass consumed by the brood for each individual carcass. Average larval weight for each carcass and total number of larvae per brood were divided by the biomass of the corresponding consumed carcass, to calculate average larval weight per gram of consumed carcass.

Statistical Analysis

Statistical analysis were performed in R version 3.4.2. Heatmaps to compare the relative abundance of bacterial and fungal taxa were plotted using lattice (12) and RColorBrewer (21) in R. Transcript abundance data was visualized using Multidimensional Scaling (MDS) plots in R using *edgeR* (22) and *limma* (23) packages. Data were filtered to include those reads that had counts per million (CPM) values greater than 1 for at least three samples in the dataset. This was done separately for the eukaryotic and prokaryotic datasets. The samples were then normalized for different library sizes using the TMM (weighted trimmed mean of M-values) method. A two-dimensional MDS scatterplot was then plotted using log2-fold change method. Data on larval development in carcass-control and carcass-removed groups was compared using a two-sample Student's t-test in R.

References for Supporting Information

1. Caporaso JG, *et al.* (2010) QIIME allows analysis of high-throughput community sequencing data. *Nat Methods* 7(5):335-336.
2. Callahan BJ, *et al.* (2016) DADA2: high-resolution sample inference from Illumina amplicon data. *Nat Methods* 13(7):581.
3. Katoh K & Standley DM (2013) MAFFT multiple sequence alignment software version 7: improvements in performance and usability. *Mol Biol Evol* 30(4):772-780.
4. Price MN, Dehal PS, & Arkin AP (2010) FastTree 2–approximately maximum-likelihood trees for large alignments. *PLoS One* 5(3):e9490.
5. Lozupone C & Knight R (2005) UniFrac: a new phylogenetic method for comparing microbial communities. *Appl Environ Microbiol* 71(12):8228-8235.
6. Lozupone CA, Hamady M, Kelley ST, & Knight R (2007) Quantitative and qualitative β diversity measures lead to different insights into factors that structure microbial communities. *Appl Environ Microbiol* 73(5):1576-1585.
7. DeSantis TZ, *et al.* (2006) Greengenes, a chimera-checked 16S rRNA gene database and workbench compatible with ARB. *Appl Environ Microbiol* 72(7):5069-5072.
8. Vázquez-Baeza Y, Pirrung M, Gonzalez A, & Knight R (2013) EMPeror: a tool for visualizing high-throughput microbial community data. *Gigascience* 2(1):16.
9. Mandal S, *et al.* (2015) Analysis of composition of microbiomes: a novel method for studying microbial composition. *Microb Ecol Health Dis* 26(1):27663.
10. Martin M (2011) Cutadapt removes adapter sequences from high-throughput sequencing reads. *EMBnet journal* 17(1):pp. 10-12.
11. Kõljalg U, *et al.* (2005) UNITE: a database providing web-based methods for the molecular identification of ectomycorrhizal fungi. *New Phytol* 166(3):1063-1068.
12. Sarkar D (2010) lattice: lattice graphics. R package version 0.18-3).
13. R Development Core Team (2013) R: A language and environment for statistical computing (R Foundation for Statistical Computing, Vienna, Austria).
14. Hausner G, Reid J, & Klassen G (1993) On the subdivision of *Ceratocystis* s.I., based on partial ribosomal DNA sequences. *Canadian Journal of Botany* 71(1):52-63.
15. Vilgalys R & Hester M (1990) Rapid genetic identification and mapping of enzymatically amplified ribosomal DNA from several *Cryptococcus* species. *J Bacteriol* 172(8):4238-4246.
16. Gibson CM & Hunter MS (2009) Inherited fungal and bacterial endosymbionts of a parasitic wasp and its cockroach host. *Microb Ecol* 57(3):542-549.
17. Kaltenpoth M & Steiger S (2014) Unearthing carrion beetles' microbiome: characterization of bacterial and fungal hindgut communities across the Silphidae. *Mol Ecol* 23(6):1251-1267.
18. Vogel H, *et al.* (2017) The digestive and defensive basis of carcass utilization by the burying beetle and its microbiota. *Nat Commun* 8:15186.
19. Kanehisa M, Furumichi M, Tanabe M, Sato Y, & Morishima K (2016) KEGG: new perspectives on genomes, pathways, diseases and drugs. *Nucleic Acids Res* 45(D1):D353-D361.
20. Hanczko R, Kőrös Á, Toth F, & Molnar-Perl I (2005) Behavior and characteristics of biogenic amines, ornithine and lysine derivatized with the o-phthalaldehyde–ethanethiol–fluorenylmethyl chloroformate reagent. *J Chromatogr A* 1087(1-2):210-222.
21. Neuwirth E (2014) RColorBrewer: ColorBrewer palettes. R package version 1.1-2.
22. Robinson MD, McCarthy DJ, & Smyth GK (2010) edgeR: a Bioconductor package for differential expression analysis of digital gene expression data. *Bioinformatics* 26(1):139-140.
23. Smyth GK (2005) Limma: linear models for microarray data. *Bioinformatics and computational biology solutions using R and Bioconductor*, eds Gentleman R, Carey V, Huber W, Irizarry R, & Dudoit S (Springer, New York), pp 397-420.